Electronic Supplementary Material (ESI) for Physical Chemistry Chemical Physics.

SUPPORTING INFORMATION

Femtosecond 2DIR spectroscopy of the nitrile stretching vibration of thiocyanate anions in liquid-to-supercritical heavy water. Spectral diffusion and libration-induced hydrogen-bond dynamics

Denis Czurlok, Michael von Domaros, Martin Thomas, Jeannine Gleim, Jörg Lindner, Barbara Kirchner, and Peter Vöhringer*

Institut für Physikalische und Theoretische Chemie, Rheinische Friedrich-Wilhelms-Universität, Wegelerstraße 12, 53115 Bonn, Germany, p.voehringer@uni-bonn.de

To judge the quality of our QM/MM Model, we performed a single AIMD simulation at 350 K, which shall be described here. We also provide further simulation results, such as densities, basic structural quantities and the remaining spectra that were not shown in the article.

1. Ab Initio Molecular Dynamics Simulations

We performed an AIMD simulation of a single thiocyanate anion dissolved in 128 heavy water molecules using the CP2k program package.[1,2] Density functional theory was used as electronic structure method, utilizing the BLYP exchange-correlation functional[3,4] with Grimme's dispersion correction D3.[5] The molecularly optimized double-zeta basis set (MOLOPT-DZVP-SR-GTH)[6] was applied to all atoms together with the corresponding Goedecker–Teter–Hutter pseudopotentials[7-9] and a plane wave cutoff of 280 Ry. A timestep of 0.5 fs was chosen, and the temperature was adjusted by a Nosé–Hoover chain thermostat. A production run of 60 ps was performed in the NVT ensemble at 350 K with a box volume corresponding to the experimental density of 1.132 g/cm^3. Molecular dipole moments were obtained by a Voronoi tessellation of the electron density[10] which was gathered during the first 30 ps.

Our QM/MM simulations were equilibrated at the experimental conditions using a Berendsen barostat with a relaxation time of 2 ps. Density averaging was performed for 1 ns. Afterwards, the simulation cell was changed to a cubic box with edges corresponding to the calculated densities. The system was allowed to equilibrate in this new environment for at least 200 ps. The final densities are shown in Table S1 together with our experimental results. Simulations are in very good agreement with the experiment for temperatures below ~ 400 K, from where on the simulated densities start deviating up to -10 %. Although this is quite large given the incompressible nature of water, we still consider these values acceptable, keeping in mind the simplicity of our water model. Since determining a density requires very long simulation runs, the AIMD was set up at the experimental density.

Table S1: Calculated and experimental number densities, n, including the thiocyanate anion.

T / K	**n_{calc} / mol cm^{-3}**	**n_{exp} / mol cm^{-3}**
293	57	56.03
333	56	55.24
350	55	54.73
393	53	53.12
453	49	50.20
513	45	46.43
573	39	41.47
633	30	33.65

TableS2: Separations of the sulfur-oxygen and nitrogen-oxygen pairs, r_{min} , at the first minimum of the corresponding RDF and average neighbor counts, <N>, within the solvation shell.

T / K	**$r_{SO,min}$ / pm**	**$r_{NO,min}$ / pm**	**$\langle N_S \rangle$**	**$\langle N_N \rangle$**
294	386	484	4.9	2.8
333	395	489	5.3	2.9
350	393	479	5.2	2.8
393	411	493	5.9	2.7
453	419	501	6.0	3.1
513	420	515	5.5	2.9
573	430	545	5.5	2.4
633	430	560	4.6	3.7

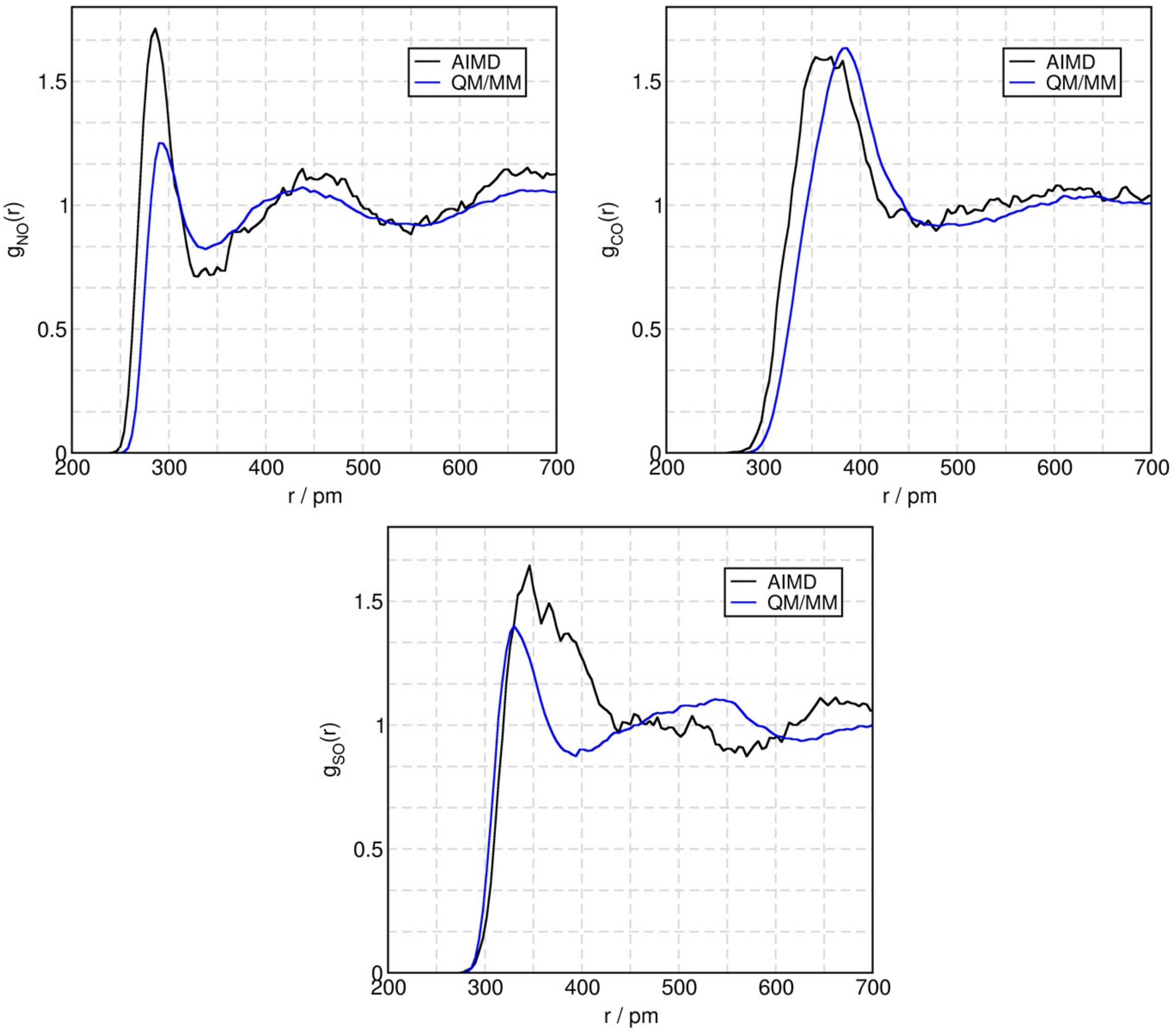

Figure S1: RDFs of the sulfur-oxygen, carbon-oxygen, and nitrogen-oxygen pairs at 350 K.

2. Structure

2.1 Radial Distribution Functions

A simple test for the quality of our QM/MM model are radial distribution functions (RDFs) which we present here for the sulfur-oxygen, carbon-oxygen, and nitrogen-oxygen pairs at 350 K, compared to our AIMD results (Fiigure S1). There is relatively good agreement between both calculations in terms of peak locations of the carbon-oxygen and nitrogen-oxygen radial pair distribution functions, which puts our definition of the solvation shell based on these functions on solid ground. Unfortunately, sulfur-oxygen RDFs perform rather poorly. Nevertheless, systematic trends within the model may still provide useful information about the molecular mechanisms investigated in the article.

Since we are interested in solvation shell and hydrogen bond dynamics, we need to define criteria that classify water molecules accordingly. We choose a geometric cutoff criterion based on the first minimum separation of the sulfur-oxygen and nitrogen-oxygen RDFs for the solvation shell around the sulfur and nitrogen atoms, respectively. The necessary cutoff values, as well as average neighbor counts obtained by integration of the RDFs are summarized in Table S2. To reduce the influence of statistical noise on the determination of the minima, histograms were smoothed using a running average prior to the determination of the minimum.

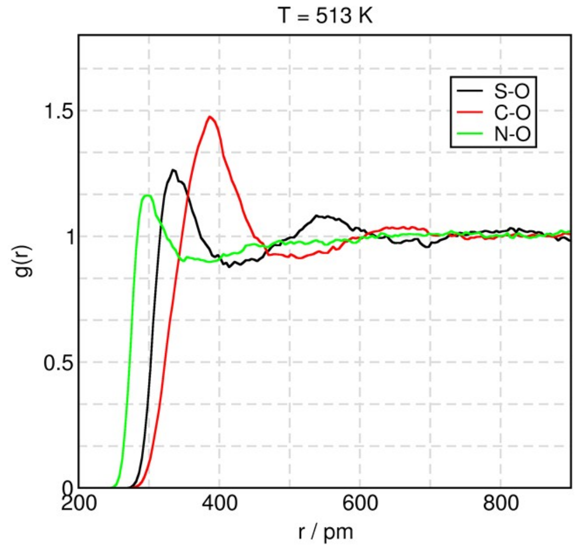

Figure S2: RDFs of the sulfur-oxygen, carbon-oxygen, and nitrogen-oxygen pairs at 350 K

The RDFs become broader and less structured with increasing temperature. Since these distribution functions are related to the potential of mean force (PMF) via $g(r) = exp(-\mathrm{PMF}(r)/kT)$, they can be used to explain the different degree of weakening of hydrogen bonds that we observe in the article: sulfur bonds were found to live almost twice as long as nitrogen bonds at high temperatures. In Figure S2, we show the different RDFs at 513 K. The nitrogen-oxygen RDF almost completely lacks the second maximum, which explains the easy breaking and associated short life time of the nitrogen HB.

Note, that the radial pair distributions obtained by our AIMD simulations qualitatively reflect the relative proton-donor strengths of thiocyanic acid (HSCN) and of its isoform (SCNH).[11] The nitrogen-oxygen contact is much more structured than its sulfur-oxygen counterpart. This indicates a relatively stronger attractive interaction between water and the nitrogen atom, or alternatively a relatively stronger proton donor capability of the thiocyanic acid.

2.2 Combined Distribution Functions

In order to define hydrogen bonds, we employ a geometrical criterion based on the combined distribution function (CDF, joint probability) of the hydrogen bond distance $r_{\mathrm{D—Acceptor}}$ and the hydrogen bond angle $\angle_{\mathrm{O–D—Acceptor}}$. Since these two-dimensional histograms are subject to much more statistical noise, than the one-dimensional RDFs, and because visualizing differences in these plots is difficult, we show only results obtained from our QM/MM simulations (Figure S3). As seen in the CDFs, the location of the global maximum does not change appreciably with temperature. We identify this maximum as the result of hydrogen bonding and use its location for the definition of the binary hydrogen bond operator h. We choose $r_{\mathrm{cut,SO}} = 320$ pm and $\angle_{\mathrm{cut,SDO}} = 120°$ and $r_{\mathrm{cut,NO}} = 240$ pm and $\angle_{\mathrm{cut,NDO}} = 130°$.

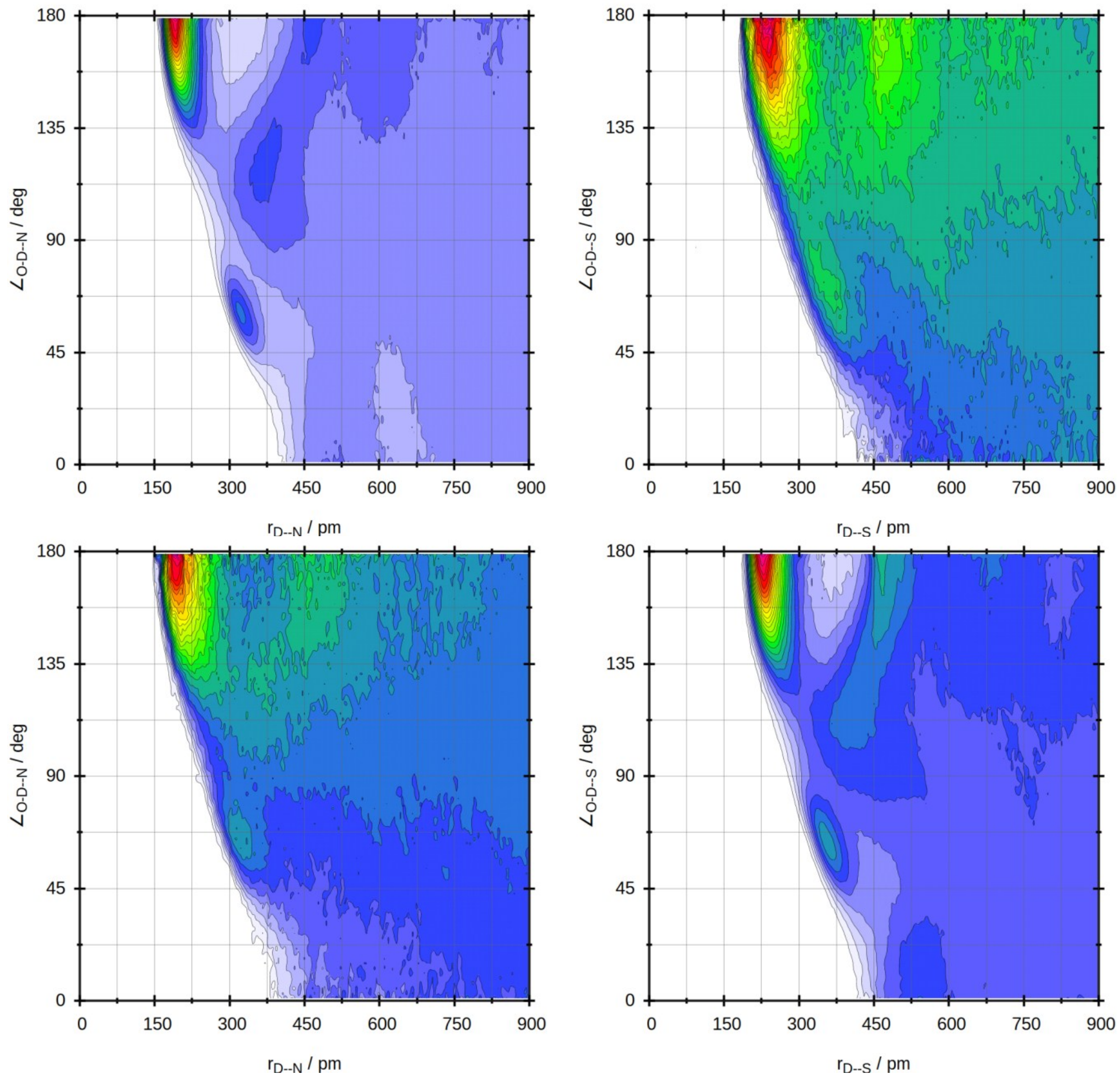

Figure S3: CDFs of the hydrogen bond distance $r_{\mathrm{D—Acceptor}}$ and the hydrogen bond angle $\angle_{\mathrm{O–D—Acceptor}}$ at 294 K (top) and 633 K (bottom). The color gradient indicates growing probability from blue via green to red.

3. Dynamics

3.1 Hydrogen Bond Dynamics

We use the geometric criteria identified above to define the hydrogen bond operator h, which equals 1 if $r_{\text{D—Acceptor}} < r_{\text{cut}}$ and $\angle_{\text{O–D—Acceptor}} > \angle_{\text{cut}}$, and is zero otherwise. Since there are much more possible water-thiocyanate pairs then hydrogen bonds between them, $\langle h \rangle \sim 0$, which leads to a simplified definition of the hydrogen bond time correlation function $c(t) = \langle \delta h(0) \delta h(t) \rangle = \langle h(0) h(t) \rangle$. If these functions decayed mono-exponentially (i.e, if there was only one dominating dynamic process on this timescale), the exponential decay constant would be the hydrogen-bond lifetime. Unfortunately, hydrogen-bond time correlation functions typically decay non-mono-exponentially, exhibiting a broad range of timescales, as different dynamic processes such as diffusion are coupled to hydrogen bond formation and breaking[12]. Instead of identifying and eliminating all relevant processes, we simply report the integral over c(t) as *characteristic time scale* τ_{HB} of hydrogen bond life. Note that these timescales are also susceptible to the definition of the hydrogen bond[12]. To eliminate statistical noise at large correlation times, hydrogen bond time correlation functions were first fitted to a sum of four exponentials and then integrated analytically. The integrals are given in the article. Here we show the time correlation functions for completeness's' sake (Figure S4).

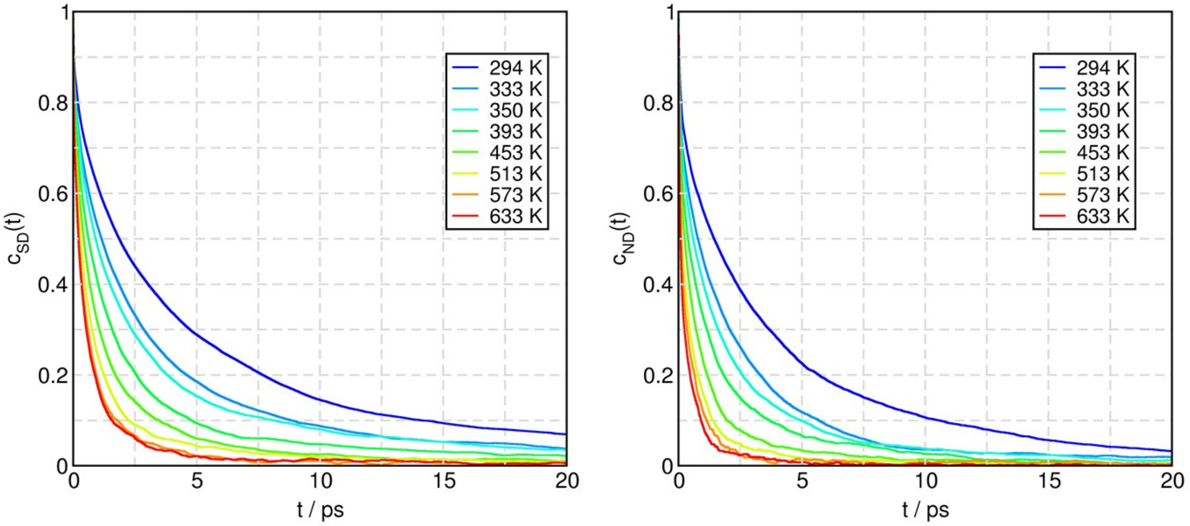

Figure S4: Hydrogen bond time correlation functions c(t) for both hydrogen bond acceptors at all investigated temperature. The color gradient indicates increasing temperature form blue via green to red.

3.2 Infrared Spectra

Infrared spectra of all heavy water molecules were calculated by Fourier Transform of the dipole-dipole orientational time correlation function. Since a rigid water model does not exhibit stretching and bending modes, we focus on the librations only. The location of that peak changes with increasing temperature from 470 cm^{-1} to 310 cm^{-1}. There are no appreciable differences to pure bulk spectra of SPC/HW (Figure S5). Apart from the missing nodes, the QM/MM spectrum compares quite well with the AIMD spectrum in terms of peak location. The different intensity can be explained with the increased permanent dipole moment which is common for effective pair potentials such as SPC/HW.[13]

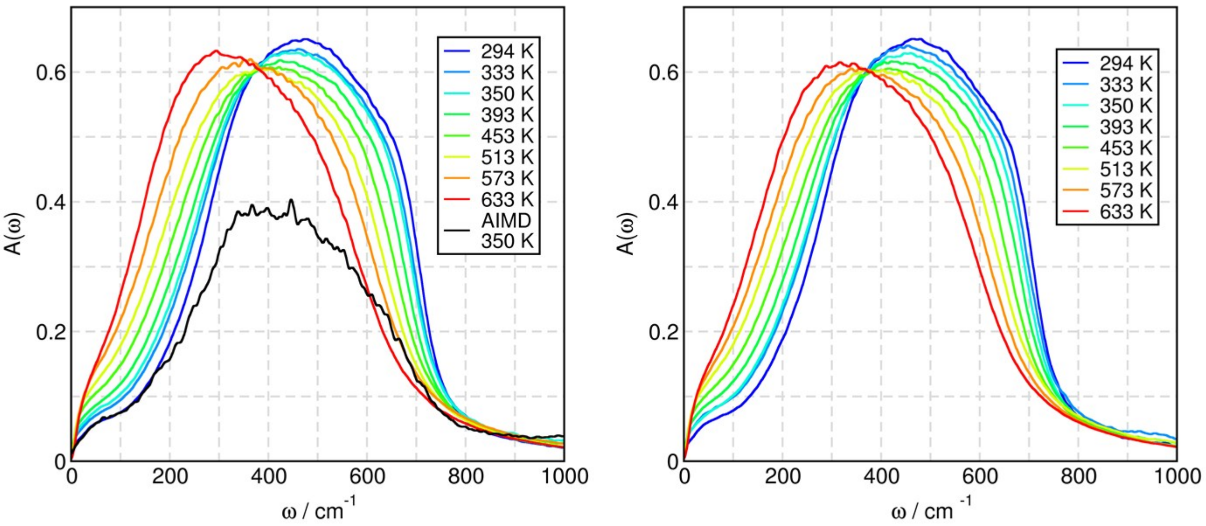

Figure S4: Left panel: IR spectrum of the SCN/heavy water system (both QM/MM and AIMD). Right panel: IR spectrum of the pure bulk water simulations.

REFERENCES

1. VandeVondele, J. et al. Quickstep: Fast and accurate density functional calculations using a mixed Gaussian and plane waves approach. *Computer Physics Communications* 167, 103-128 (2005).

2. Hutter, J., Iannuzzi, M., Schiffmann, F. and VandeVondele, J. cp2k: atomistic simulations of condensed matter systems. *WIREs Comput Mol Sci* 4, 15-25 (2013).

3. Becke, A. Density-functional exchange-energy approximation with correct asymptotic behavior. *Physical Review A* 38, 3098-3100 (1988).

4. Lee, C., Yang, W. and Parr, R. Development of the Colle-Salvetti correlation-energy formula into a functional of the electron density. *Physical Review B* 37, 785-789 (1988).

5. Grimme, S., Antony, J., Ehrlich, S. and Krieg, H. A consistent and accurate ab initio parametrization of density functional dispersion correction (DFT-D) for the 94 elements H-Pu. *J. Chem. Phys.* 132, 154104 (2010).

6. VandeVondele, J. and Hutter, J. Gaussian basis sets for accurate calculations on molecular systems in gas and condensed phases. *J. Chem. Phys.* 127, 114105 (2007).

7. Goedecker, S., Teter, M. and Hutter, J. Separable dual-space Gaussian pseudopotentials. *Physical Review B* 54, 1703-1710 (1996).

8. Hartwigsen, C., Goedecker, S. and Hutter, J. Relativistic separable dual-space Gaussian pseudopotentials from H to Rn. *Physical Review B* 58, 3641-3662 (1998).

9. Krack, M. Pseudopotentials for H to Kr optimized for gradient-corrected exchange-correlation functionals. *Theoretical Chemistry Accounts* 114, 145-152 (2005).

10. Thomas, M., Brehm, M. and Kirchner, B. Voronoi dipole moments for the simulation of bulk phase vibrational spectra. *Phys. Chem. Chem. Phys.* 17, 3207-3213 (2015).

11. Pankratov, A.N. and Khmelev, S.S. Protolytic properties of cynaic and thiocyanic acids and their isoforms. *J. Struct. Chem.* 46, 404-408 (2005).

12. Luzar, A. and Chandler, D. Hydrogen-bond kinetics in liquid water. *Nature* 379, 55-57 (1996).

13. Berendsen, H., Grigera, J. and Straatsma, T. The missing term in effective pair potentials. *J. Phys. Chem.* 91, 6269-6271 (1987).